

Supporting Information

Vertically-oriented Self-assembly of Colloidal CdSe/CdZnS Quantum Wells Controlled via Hydrophilicity/Lipophilicity Balance: Optical Gain of Quantum Well Stacks for Amplified Spontaneous Emission to Random Lasing

Zeynep Dikmen^{a,b}, Ahmet Tarık Işık^a, İklim Bozkaya^a, Hamed Dehghanpour Baruj^a, Betül Canımurbey^{a,c}, Farzan Shabani^a, Muhammad Ahmad^a, and Hilmi Volkan Demir^{a,d}

^aFaculty of Engineering, Department of Biomedical Engineering, Eskisehir Osmangazi University, 26040 Eskisehir, Turkey

^bDepartment of Electrical and Electronics Engineering, Department of Physics, UNAM – Institute of Materials Science and National Nanotechnology Research Center, Bilkent University, Ankara 06800, Turkey

^cAmasya University, Sabuncuoglu Şerefeddin Health Services Vocational School, 05100, Amasya, Turkey
Amasya University, Central Research Laboratory, 05100, Amasya, Turkey

^dLUMINOUS! Centre of Excellence for Semiconductor Lighting and Displays, School of Electrical and Electronic Engineering, School of Physical and Mathematical Sciences, School of Materials Science and Engineering, Nanyang Technological University, 50 Nanyang Avenue, 639798, Singapore

*E-mail to: volkan@bilkent.edu.tr

Prof. H. V. D.

LUMINOUS! Centre of Excellence for Semiconductor Lighting and Displays

Centre of Optical Fiber Technology

The Photonics Institute

School of Electrical and Electronic Engineering

School of Physical and Mathematical Sciences

Nanyang Technological University

50 Nanyang Avenue, Singapore 639798, Singapore

*E-mail: hvdemir@ntu.edu.sg

Synthesis of CdSe/CdZnS

Materials: Sodium myristate ($\geq 99.0\%$), cadmium acetate ($\text{Cd}(\text{OAc})_2$, 99.995%), cadmium acetate dihydrate ($\text{Cd}(\text{OAc})_2 \cdot 2\text{H}_2\text{O}$, 98%), zinc acetate ($\text{Zn}(\text{OAc})_2$, 99.99%), selenium (99.99%), sulfur (99.98%), 1-octanethiol ($\geq 98.5\%$), oleic acid (OA, 90%), oleylamine (OLA, 70%), 1-octadecene (ODE, 90%), ethylene glycol (99.8%), diethylene glycol (99%), sodium dodecylsulfate ($\geq 99.0\%$), cetyltrimethylammonium bromide (98%), n-hexane ($\geq 97.0\%$), ethanol (absolute), methanol ($\geq 99.7\%$) and toluene ($\geq 99.5\%$) were purchased from Sigma Aldrich, and used without any purification.

Cadmium(myristate)₂ synthesis: $\text{Cd}(\text{myr})_2$ was synthesized according to literature with minor modifications [1]. 1.23 g cadmium nitrate was dissolved in 40 mL of methanol followed by mixing 3.13 g of sodium myristate dissolved in 250 mL of methanol by stirring for 1 h. The synthesized white precipitate was filtered and dried under vacuum overnight.

4 ML CdSe CQWs core synthesis: CdSe CQWs were synthesized according to the slightly modified recipe from the literature [1]. 346 mg $\text{Cd}(\text{myr})_2$, 24 mg Se powder and 30 mL ODE were put in a three-neck flask and degassed under vacuum at room temperature for 1 h and at 95 °C for 30 min. The temperature was increased to 235 °C under nitrogen flow. 126 mg cadmium acetate dihydrate ($\text{Cd}(\text{OAc})_2 \cdot 2\text{H}_2\text{O}$) was added when the temperature reached at 195 °C and the color is bright yellow.

The mixture was stirred for 10 min at 235 °C followed by quenching in a water bath and addition of 1 mL oleic acid right after quenching. When the temperature decreased to room temperature, 10 mL hexane was added and side products such as quantum dots or 5 ML CdSe COWs forming simultaneous were removed by selective precipitation at 6000 rpm for 6 minutes with hexane and ethanol.

CdSe/CdZnS core/HL shell CQWs synthesis: 4 mL CdSe CQWs core solution (optical density of 4 at 350 nm) was precipitated by centrifugation after ethanol addition. The precipitated core was redispersed in hexane and put in 50 mL three-neck flask. 22 mg Cd(OAc)₂ and 75 mg Zn(OAc)₂, 1 mL OA and 7.5 mL ODE were added into the flask and the mixture was degassed at room temperature for 30 minutes and 95 °C for 1 hour followed by flushing the flask with nitrogen gas. 1 mL of OLA was added to the solution at 95 °C, and the mixture was heated up to 300 °C. 1-octanethiol solution in ODE (350 μL octanethiol in 15 mL ODE) injection with the rate of 10 mL/h was started into the solution around 162 °C and at the rate of injection was decreased to 4 mL/h at 240 °C. 4 mL of sulphur resource was injected till temperature reached to 300 °C. The mixture was stirred at 300 °C till required emission wavelength was observed by PL measurement. Then, the reaction was quenched in a water bath at room temperature and the product was centrifuged after 10 mL of hexane addition to purify the CQWs from the unstable particles. The CQWs were separated from the unwanted species by selective precipitation with ethanol and hexane.

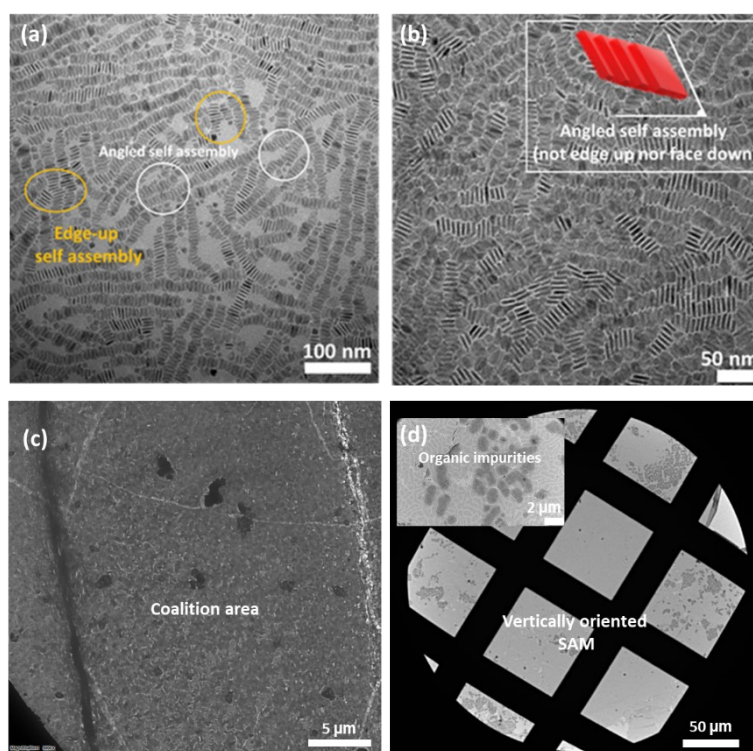


Figure S1. TEM micrographs of CdSe/CdZnS stacks and angled stacks formation (a,b) coalition area (c), SAM layer (d) .

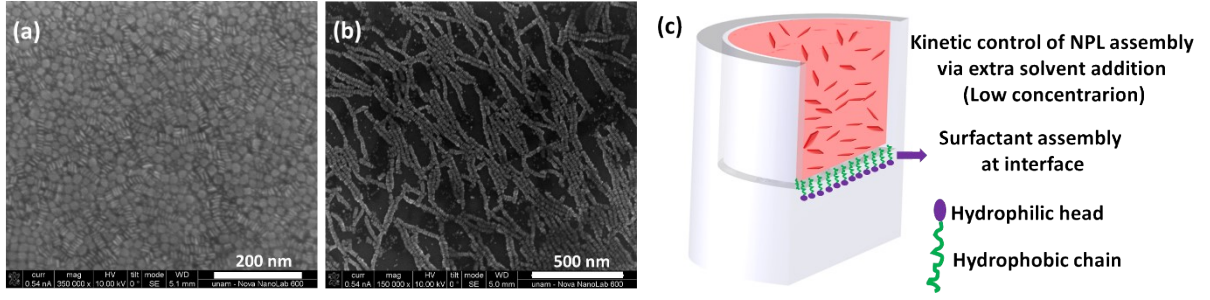


Figure S2. SEM micrograph of CdSe/CdZnS stacks formation affected by surfactant addition: SDS containing EG subphase (a). CTAB containing EG subphase (b). Illustration of surfactant assembly on the subphase (c).

Back Focal Plane Imaging

To analyze the k-space-dependent emission, we used an inverted optical microscope (Nikon eclipse Ti-U) equipped with a charge-coupled device (CCD) camera (Thorlabs). The sample was excited and collected via quartz substrate using an oil-immersed high numerical aperture (NA) objective lens of 1.3. The setup we employed is shown schematically in Fig. S3.

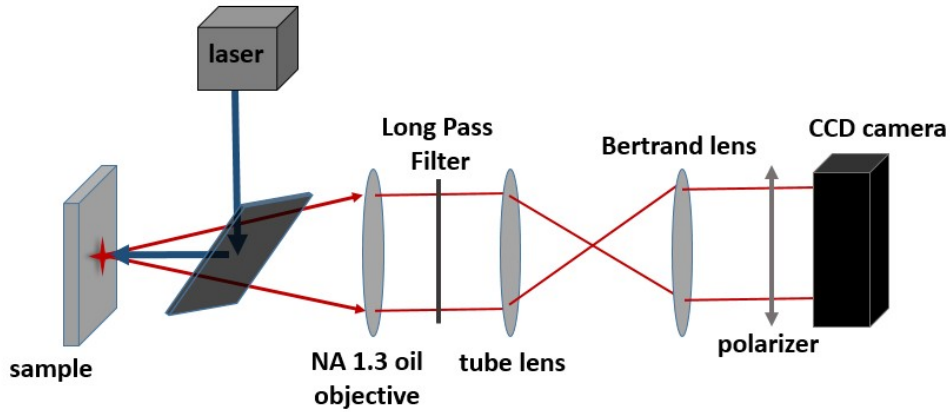


Figure S3. Schematic representation of back focal plane imaging.

Theoretical derivations

To investigate back focal plane imaging simulations, we followed the work of Schuller et al. [2] and Scott et al.[3] which offers thorough details about the derivation of model. In the three-layer structure of air, nanoplatelets, and a substrate as illustrated in Fig. S4, the reflection and transmission of a plane wave between interfaces is described by the Fresnel equations,

$$t_{ij}^p = \frac{2n_i n_j k_{zi}}{n_j^2 k_{zi} + n_i^2 k_{zi}}, \quad t_{ij}^s = \frac{2k_{zi}}{k_{zi} + k_{zj}}, \quad (\text{S1})$$

$$(\text{S2})$$

$$r_{ij}^p = \frac{n_j^2 k_{zi} - n_i^2 k_{zj}}{n_j^2 k_{zi} + n_i^2 k_{zj}}, \quad r_{ij}^s = \frac{k_{zi} - k_{zj}}{k_{zi} + k_{zj}},$$

where the symbols s and p signify the polarization of the electromagnetic wave with regard to the plane of incidence, while n and k denote the refractive index and momentum, respectively.

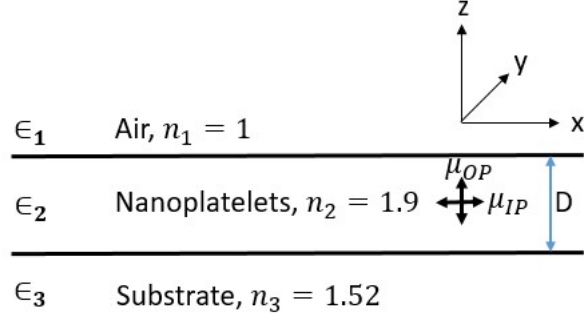


Figure S4. Schematic illustration of the three-layer structure.

A combination of reflection on the interfaces and interference inside the emitter layer defines the local density of optical states (LDOS) for in-plane (IP) and out-of-plane (OP) dipoles producing s and p polarized light in the configuration of the three layers. The LDOS is determined as follows:

$$\rho_{IP}^s = p_x^s(k_x, k_y) = \left(\frac{1}{8\pi k_0^2} \right) \left(\frac{k_0}{k_{z3}} \right) \left| \frac{t_{32}^s e^{\frac{ik_{z2}D}{2}} \left(1 + r_{21}^s e^{\frac{2ik_{z2}D}{2}} \right) k_y}{1 - r_{21}^s r_{23}^s e^{2ik_{z2}D} \sqrt{k_x^2 + k_y^2}} \right|^2$$

$$\rho_{IP}^p = p_x^p(k_x, k_y) = \left(\frac{1}{8\pi k_0^2} \right) \left(\frac{k_0}{k_{z3}} \right) \left| \frac{t_{32}^p e^{\frac{ik_{z2}D}{2}} \frac{k_{z2}}{n_2 k_0} \left(1 - r_{21}^p e^{\frac{2ik_{z2}D}{2}} \right) k_x}{1 - r_{21}^p r_{23}^p e^{2ik_{z2}D} \sqrt{k_x^2 + k_y^2}} \right|^2 \quad (S3)$$

$$\rho_{OP}^p = p_z^s(k_x, k_y) = \left(\frac{1}{8\pi k_0^2} \right) \left(\frac{k_0}{k_{z3}} \right) \left| \frac{t_{32}^p e^{\frac{ik_{z2}D}{2}} \frac{k_x}{n_2 k_0} \left(1 + r_{21}^p e^{\frac{2ik_{z2}D}{2}} \right)}{1 - r_{21}^p r_{23}^p e^{2ik_{z2}D}} \right|^2$$

where D is the thickness of the emitting layer, k₀ is the total free space momentum.

The emission projected on the imaging plane in the direction of (k_x, k_y) is computed using the preceding formulae:

$$N^s(k_x, k_y) = A \rho_{IP}^s f_{IP} |\mu_{IP}|^2 \quad (S4)$$

$$N^p(k_x, k_y) = A (\rho_{IP}^p f_{IP} |\mu_{IP}|^2 + \rho_{OP}^p f_{OP} |\mu_{OP}|^2)$$

where A is a constant related to experimental conditions, f is the dipole distribution, and μ is the dipole moment.

The emission pattern can be estimated using these equations, and the dipole distribution can be extracted by fitting the calculations into the experimental results (Fig. S5).

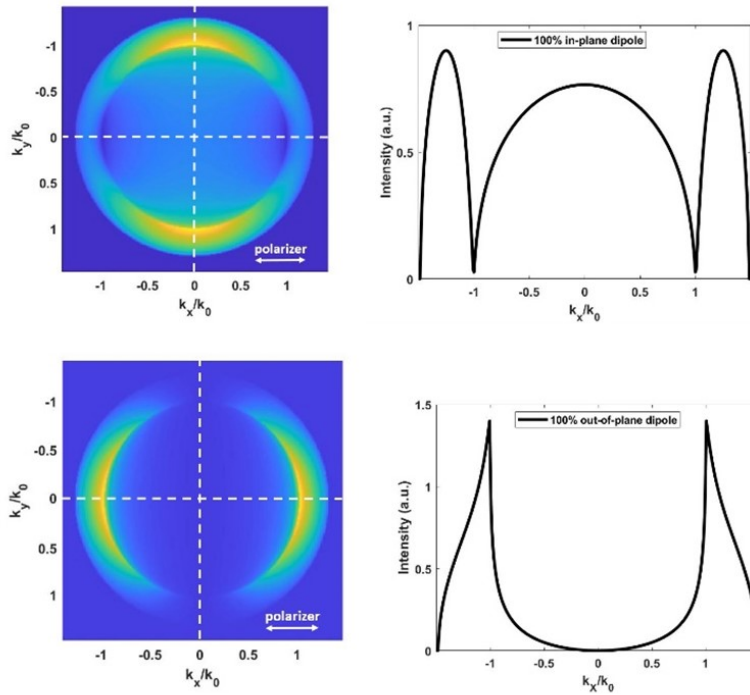


Figure S5. Emission profile (a,c) and intensity diagrams (c,d) of in-plane (IP) (up) and out-of-plane (OP) dipoles (down).

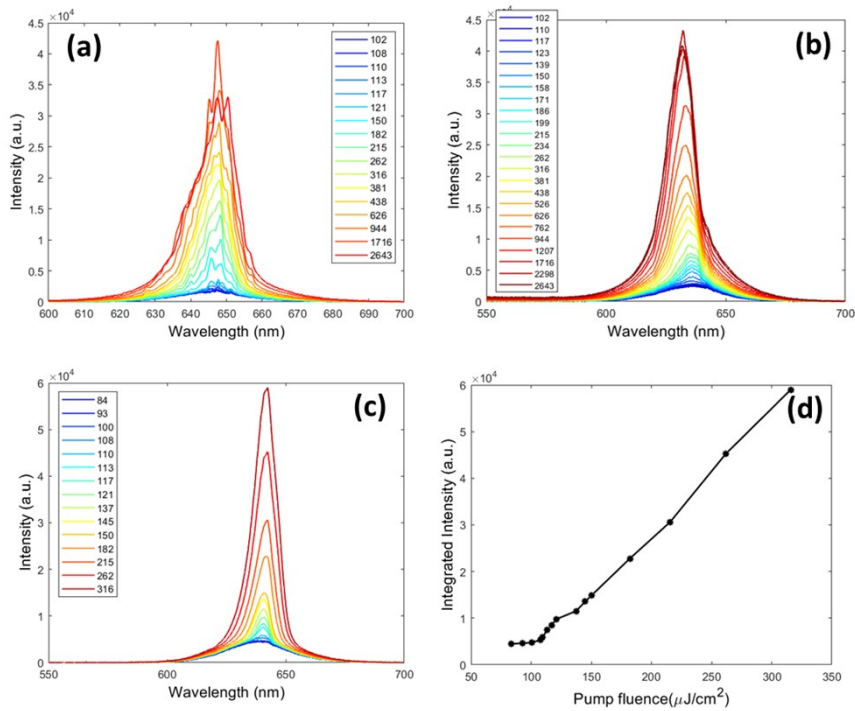


Figure S6. PL spectra evolution of the samples with different thicknesses by the pulse energy density of the pump excited with a pulsed laser at 400 nm: 1 layer of SAM CQWs (a). Sequentially deposited 2 layers of SAM CQWs (b). Sequentially deposited 4 layers of SAM CQWs (c) Integrated emission intensity of sequentially deposited 4 layers of SAM CQWs as a function of the pump fluence (d).

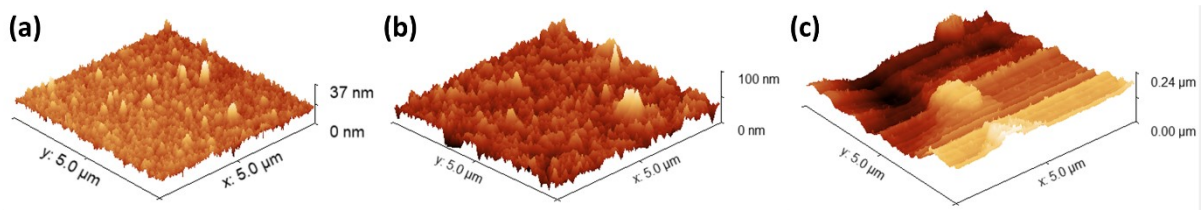


Figure S7. AFM images of sequentially deposited SAM CQWs for monolayer (a), 3 layers (b) and 10 layers (c).

References

1. Tessier, M.D., et al., *Efficient Exciton Concentrators Built from Colloidal Core/Crown CdSe/CdS Semiconductor Nanoplatelets*. *Nano Letters*, 2014. **14**(1): p. 207-213.
2. Schuller, J.A., et al., *Orientation of luminescent excitons in layered nanomaterials*. *Nature Nanotechnology*, 2013. **8**(4): p. 271-276.
3. Scott, R., et al., *Directed emission of CdSe nanoplatelets originating from strongly anisotropic 2D electronic structure*. *Nature Nanotechnology*, 2017. **12**(12): p. 1155-1160.